Primates (2016) 57:541–547
DOI 10.1007/s10329-016-0546-y

ORIGINAL ARTICLE

# Primate genotyping via high resolution melt analysis: rapid and reliable identification of color vision status in wild lemurs

**Rachel L. Jacobs[1,2,3] · Amanda N. Spriggs[1,4] · Tammie S. MacFie[5] · Andrea L. Baden[3,6,7,8] · Mitchell T. Irwin[9] · Patricia C. Wright[3,10] · Edward E. Louis Jr.[11] · Richard R. Lawler[12] · Nicholas I. Mundy[5] · Brenda J. Bradley[1]**

Received: 6 March 2016 / Accepted: 13 May 2016 / Published online: 6 June 2016


**Abstract** Analyses of genetic polymorphisms can aid our understanding of intra- and interspecific variation in primate sociality, ecology, and behavior. Studies of primate opsin genes are prime examples of this, as single nucleotide variants (SNVs) in the X-linked opsin gene underlie variation in color vision. For primate species with polymorphic trichromacy, genotyping opsin SNVs can generally indicate whether individual primates are red-green color-blind (denoted homozygous M or homozygous L) or have full trichromatic color vision (heterozygous ML). Given the potential influence of color vision on behavior and fitness, characterizing the color vision status of study subjects is becoming commonplace for many primate field projects. Such studies traditionally involve a multi-step sequencing-based method that can be costly and time-consuming. Here we present a new reliable, rapid, and relatively inexpensive method for characterizing color vision in primate populations using high resolution melt analysis (HRMA). Using lemurs as a case study, we characterized variation at exons 3 and/or 5 of the X-linked opsin gene for 87 individuals representing nine species. We scored opsin genotypes and color vision status using both traditional sequencing-based methods as well as our novel melting-curve based HRMA protocol. For each species, the melting curves of varying genotypes (homozygous M, homozygous L, heterozygous ML) differed in melting temperature and/or shape. Melting curves for each sample were consistent across replicates, and genotype-specific melting curves were consistent across DNA sources (blood vs. feces). We show that opsin genotypes can be quickly and reliably scored using HRMA once lab-specific reference curves have been developed based on known genotypes. Although the protocol presented here focuses on genotyping lemur opsin loci, we also consider the larger potential for applying this approach to various types of genetic studies of primate populations.

✉ Rachel L. Jacobs
rachel_jacobs@gwu.edu

✉ Brenda J. Bradley
bradleyjbrenda@gwu.edu

[1] Department of Anthropology, Center for the Advanced Study of Human Paleobiology, The George Washington University, Washington, DC, USA

[2] Interdepartmental Doctoral Program in Anthropological Sciences, Stony Brook University, Stony Brook, USA

[3] Centre ValBio Research Station, Ranomafana, Fianarantsoa, Madagascar

[4] Department of Anthropology, University at Albany-SUNY, Albany, USA

[5] Department of Zoology, University of Cambridge, Cambridge, UK

[6] Department of Anthropology, Hunter College of City University of New York, New York, USA

[7] Departments of Anthropology and Biology, The Graduate Center of City University of New York, New York, USA

[8] The New York Consortium in Evolutionary Primatology, New York, USA

[9] Department of Anthropology, Northern Illinois University, DeKalb, USA

[10] Department of Anthropology, Stony Brook University, Stony Brook, USA

[11] Conservation Genetics Department, Omaha's Henry Doorly Zoo and Aquarium, Omaha, USA

[12] Department of Sociology and Anthropology, James Madison University, Harrisonburg, USA

**Keywords** Opsin · Strepsirrhines · Sensory ecology · Technique · Single nucleotide variant genotyping

## Introduction

Unlike most mammals, many primates are able to readily distinguish between colors of long wavelength light (oranges and reds) and medium wavelength light (greens) (Jacobs 1993). This capacity for trichromatic color vision results from individuals having three functional cone photoreceptors in the retina that are tuned to different spectral sensitivities: short (S), medium (M), and long (L) wavelengths (Neitz et al. 1991; Jacobs 1995; Dacey 2000). This spectral tuning is determined by differences in photopigment opsin proteins, which are coded by opsin genes (Jacobs 1995; Surridge et al. 2003).

Most primates have a functional copy of the autosomal S opsin gene, but many species differ in the presence and spectral tuning of X-linked M and L opsins, resulting in differences in color vision capacities (Jacobs 1995; Tan and Li 1999). Virtually all catarrhines have trichromatic color vision due to a duplication of the X-linked opsin gene, with the two gene copies separately encoding M and L proteins (Dulai et al. 1999). Malagasy lemurs and most Neotropical monkeys, however, have a single X-linked opsin gene, and this gene is often variable, with M and L opsins as possible allelic variants (Jacobs 1998; Tan and Li 1999; Jacobs and Deegan 2003). Heterozygous females with two different variants (M and L) have the potential for trichromatic color vision, while males and homozygous females are red-green color-blind (dichromatic for only M or only L) (Jacobs 1998; Tan and Li 1999).

Differences in the spectral sensitivity of M and L opsins are largely due to nonsynonymous substitutions at a few key codon sites in the X-linked opsin gene (Nathans et al. 1986; Tovee 1994; Shyue et al. 1998; Nathans 1999). In platyrrhines, three key amino acid sites (exon 3 site 180; exon 5 sites 277, 285) impact major spectral shifts (changes at exon 4 sites 229, 233 have additional minor effects) (Neitz et al. 1991; Yokoyama and Radlwimmer 1998). Variation in most lemurs is due to a single-site polymorphism (exon 5 site 285) (Tan and Li 1999; Veilleux and Bolnick 2009). Thus, color vision differences in many primates are due to a small number of single nucleotide variants (SNVs). Since genotype and phenotype are tightly linked (e.g., Bowmaker et al. 1980; Jacobs 1984), the color vision status of individual primates—dichromatic L, dichromatic M, or trichromatic—can be assessed by sequencing opsin genes at these diagnostic SNV sites (e.g., Melin et al. 2007, 2008; Hiramatsu et al. 2008).

Given the potential influence of color vision on behavior and fitness, characterizing the color vision status of study subjects is becoming commonplace for many primate field projects (Bunce et al. 2011; Fedigan et al. 2014; Jacobs and Bradley 2016). Several studies of wild platyrrhines have assessed the relationship between color vision and fruit foraging (Vogel et al. 2007; Hiramatsu et al. 2008; Melin et al. 2008), insect capture (Melin et al. 2007; Smith et al. 2012), activity cycle (Mundy et al. 2016), grouping patterns (Surridge et al. 2005), and fitness (Fedigan et al. 2014). Studies of wild lemurs have also examined color vision in relation to foraging, activity cycle, and ambient light (Veilleux et al. 2014; Valenta et al. 2015).

Such studies characterizing color vision via opsin genotyping generally entail targeting ~100–300-base pair (bp) exonic regions via the polymerase chain reaction (PCR), followed by Sanger sequencing and sequence alignment (e.g., Hiramatsu et al. 2005; Vogel et al. 2007; Leonhardt et al. 2009; Bunce et al. 2011). Heterozygous genotypes are identified by the presence of two nucleotide peaks at diagnostic sites on both strands (forward and reverse). Although straightforward, this multi-step approach can be time-consuming and costly, especially since most Sanger sequencing is now outsourced to core facilities. Here we present a rapid, inexpensive method for assessing color vision genotypes using high resolution melting analysis (HRMA) of PCR amplicons.

HRMA entails a quantitative PCR reaction using intercalating fluorescent dyes, followed immediately by characterization of precise amplicon melt curves showing fluorescence as a function of temperature in real time (Liew et al. 2004). HRMA takes advantage of the fact that double-stranded DNA is connected by hydrogen bonds, which can be broken by heat. The stability of a sequence changes based on the nucleotide content (e.g., A-T base pairs form two hydrogen bonds, G–C pairs form three) (Doktycz 2002). Thus, the melt temperature and shape of a melt curve is determined by the nucleotide sequence, and SNV genotypes produce sequence-specific melt curves that differ in melt temperature and/or shape (Wittwer et al. 2003).

Commonly used in clinical diagnostics (Payne et al. 2014), HRMA has considerable, yet so far underutilized, potential for studies of wild populations (Smith et al. 2010). We developed an efficient HRMA approach for assessing color vision genotypes in wild primates. We describe the protocol here and discuss its potential utility and application, as well as some considerations and limitations.

## Methods

We extracted genomic DNA from blood ($n = 75$ individuals) and fecal ($n = 13$ individuals) samples representing nine lemur species ($n = 87$ individuals total; Table 1). We

**Table 1** Lemur species, study sites, and sample sizes used in high resolution melting analysis (HRMA)

| Species | Site | $n_{\text{total ind.}}$ ($n_{\text{ind. fecal samples}}$) |
|---|---|---|
| *Eulemur rubriventer* | Ranomafana National Park | 8 |
| *Eulemur rufifrons* | Ranomafana National Park | 14 |
| *Hapalemur aureus* | Ranomafana National Park | 5 |
| *Lemur catta* | Isalo National Park | 6 |
| *Prolemur simus* | Ranomafana National Park | 3 |
| *Propithecus diadema* | Tsinjoarivo | 6 |
| *Propithecus edwardsi* | Ranomafana National Park | 24 (13) |
| *Propithecus verreauxi* | Beza Mahafaly Reserve | 2 |
| | Andohahela National Park | 6 |
| *Varecia variegata* | Ranomafana National Park | 13[a] |
| Total | | 87 (13) |

Counts represent the number of individuals (*ind.*) sequenced at exon 5 of the M/L opsin gene

[a] For *V. variegata*, 11 individuals were also sequenced at exon 3

used spin-column based extraction protocols (Qiagen DNeasy Blood and Tissue Kit and Stool Kit) following the manufacturer's instructions and automated on a QIAcube. For fecal extractions we modified the initial lysis step with an extended 48-h incubation in buffer ASL at room temperature and negative controls were included in all extractions (see also Jacobs and Bradley 2016).

We amplified exons 3 (166 bp) and 5 (240 bp) of the M/L opsin gene using quantitative (real time) PCR (qPCR). Primer pairs were originally developed for Sanger sequencing of lemur opsin loci (exon 3, 5′-TCTGGTCCC TGGCCATCATTTC-3′ and 5′-CACACTTACCTGCTCC AACC-3′; exon 5, 5′-GTAGCAAAGCAGCAGAAAGA-3′ and 5′-CTGCCGGTTCATAAAGACGTAGATAAT–3′). We carried out qPCR reactions on a Rotor-Gene Q (Qiagen) real time PCR platform. Reactions (20 µl) contained 12.50 µl of Type-it HRM MasterMix (HotStarTaq plus DNA polymerase, EvaGreen dye, Q-Solution, deoxynucleotides, and $MgCl_2$), 1.75 µl primer mix (10 mM concentration forward and reverse), and 5.0 µl of DNA template (generally $\leq$10 µg/µl; based on Nanodrop spectrophotometer measurements). We included no-template controls and blanks (water) in each qPCR run.

We set thermocycling profiles as: an initial activation at 95 °C for 5 min followed by 50 cycles of denaturing at 94 °C for 30 s, annealing at 48 °C for 40 s, and extension at 72 °C for 60 s. We generated data on the melting patterns of qPCR products immediately following amplification by increasing temperatures from 80 to 90 °C, rising by 0.1 °C/2 s. We plotted fluorescence data as a function of temperature during DNA denaturation (melting) and used the Rotor-Gene Q software package (Qiagen) to visualize and compare melting curves.

Because melting curves reflect variation in DNA sequences, we examined whether melting curves could be reliable indicators of opsin genotypes. In general, homozygotes should be distinguished from each other by variation in melt temperature, and heterozygotes distinguished by variation in melt curve shape (e.g., Liew et al. 2004). Given that most variation in lemur M/L opsins has been identified in exon 5, we generated and compared melting temperatures and curve shape for exon 5 for all 87 individuals in up to six independent qPCR and HRM analyses (mean = 2.76 replicates per sample). For a subset of *Varecia variegata* samples ($n = 11$ individuals), we also generated melting curves for exon 3, which is not known to vary in most lemur species, in a single qPCR and HRM analysis. We then assessed whether melting curve assignments accurately corresponded to true opsin genotypes based on traditional sequencing methods. That is, Sanger sequencing and HRMA results were directly compared for all samples. For most of the samples ($n = 75$ individuals) we had already generated sequence data from standard PCR (using the same primer sequences given above for qPCR) and Sanger sequencing protocols as part of a parallel study. For a subset of samples ($n = 22$ individuals) we directly sequenced the HRMA amplicons (after HRMA scoring) via traditional Sanger sequencing in both directions on an Applied Biosystems Genetic Analyzer at the DNA Analysis Facility at Yale University. Intercalating dyes like SYBR green/EvaGreen should not interfere with cycle sequencing, and our results confirm this. Based on the comparisons, we identified the idiosyncratic curve shape and melting temperature of each genotype for each species.

## Results

For each species, the melting curves of varying genotypes at exon 5 of the M/L opsin gene (homozygous M, homozygous L, heterozygous) differed in melting temperature and/or shape, and melting curves for each sample

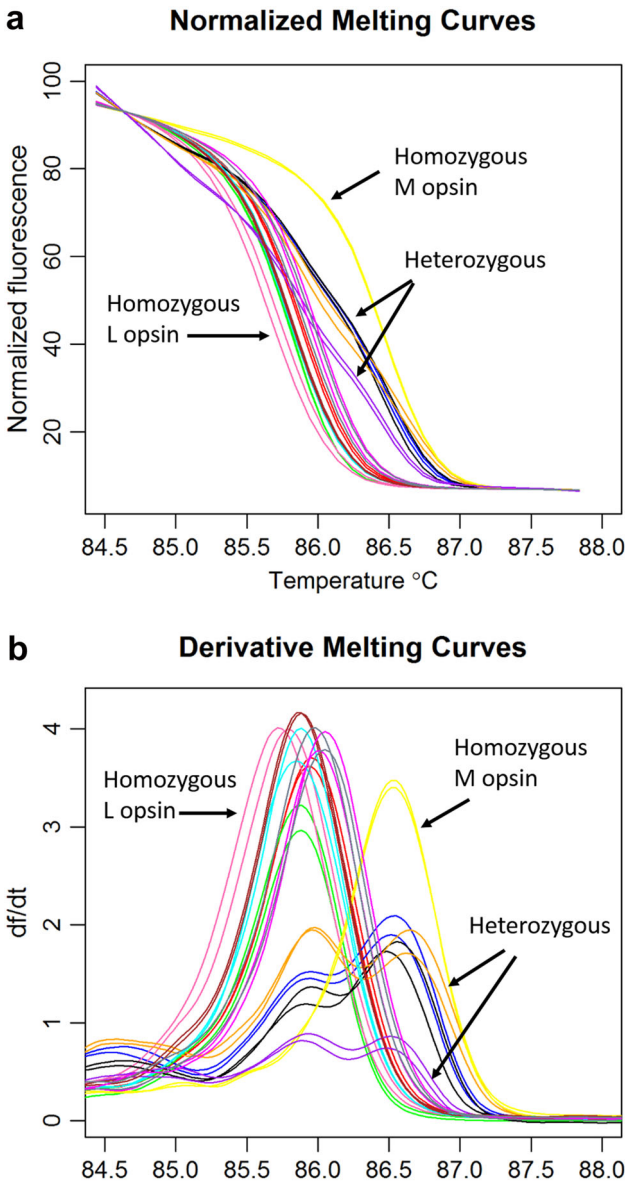


**Fig. 1** Normalized high resolution melting curves (**a**) and derivative melting curves (**b**) for exon 5 of the M/L opsin gene for *Propithecus edwardsi*. Each color represents an individual and each individual is represented by two samples revealing intra-individual consistency and inter-individual variation

were consistent across replicates (Fig. 1a). To more clearly visualize melting temperatures, we plotted derivative melting curves (Fig. 1b), and as expected, homozygous individuals exhibited a single melting curve peak, with M and L opsin variants differing in melting temperature. Heterozygous individuals showed a different melt curve shape with two melt curve peaks (Fig. 1b).

For all individuals ($n = 87$) and all replicates, those identified as homozygous or heterozygous based on Sanger sequencing trace files exhibited single-peak or double-peak melt curves, respectively. That is, our HRM analyses produced no false positives or false negatives. Melting curves were also consistent across samples derived from different DNA sources (feces and blood). Specifically, melting temperatures for different genotypes using DNA from fecal samples were captured within the melting temperature ranges of those using DNA from blood (see results for *Propithecus edwardsi* in Table 2).

For those species with color vision variation (i.e., *Propithecus diadema*, *P. edwardsi*, and *V. variegata*), the number of SNVs differing between M and L opsins varied (i.e., Sanger sequencing indicated that M and L opsins in some species differ by more than one SNV), but in all cases, heterozygotes were distinguished from homozygotes by double-peak melt curves. Furthermore, the two homozygous genotypes (i.e., homozygous M and homozygous L) could be readily distinguished by differences in melting temperature (Fig. 1a, b; Table 2). Importantly, the average and range in melting temperature for M and L opsin amplicons varied across species (Table 2). Because there was no color vision variation present in our samples for some species (e.g., *Eulemur rubriventer*, *Eulemur rufifrons*, and *Lemur catta*), the utility of this method for distinguishing potential variation in these species could not be assessed. Similarly, no variation was found in our sample of exon 3, comprising 11 *V. variegata* individuals. All samples exhibited a single melting curve peak ($n = 11$ individuals and replicates, mean = 86.04, SD = 0.10, range = 85.95–86.30).

## Discussion

Our study has identified HRMA as a useful tool for assessing color vision status in wild lemur populations. We demonstrate that melt curves of color vision genotypes consistently match results from traditional PCR and Sanger sequencing methods. Consistency extends across multiple species and using samples varying in relative DNA quality (blood, feces). Color vision genotypes (homozygous M, homozygous L, and heterozygous) could be readily differentiated based on melting curve temperature and shape in polymorphic taxa. For those species exhibiting low-level variation, HRMA may be a useful tool for initial screening of individuals to target those potentially exhibiting different color vision genotypes. Direct sequencing of HRMA amplicons can be used for confirmation.

Thus, opsin genotypes can be quickly and reliably scored using HRMA, and we make the following recommendations for implementing such a study:

1. PCR primers should flank small segments. Short PCR amplicons produce greater melting temperature differences among genotypes (Parant et al. 2009), are less

**Table 2** Peak melting temperatures (MT; °C) for exon 5 amplicons from each lemur species and M/L opsin genotype

| Species | Genotype | Color vision | Opsin | $n_{ind.}$ | Mean MT ± SD | Range |
|---|---|---|---|---|---|---|
| *Eulemur rubriventer* | Homozygote | Dichromat | L | 8 | 85.56 ± 0.14 | 85.35–85.83 |
| *Eulemur rufifrons* | Homozygote | Dichromat | M | 14 | 86.09 ± 0.66 | 85.53–87.58 |
| *Hapalemur aureus* | Homozygote | Dichromat | L | 5 | 85.72 ± 0.06 | 85.60–85.83 |
| *Lemur catta* | Homozygote | Dichromat | M | 6 | 86.12 ± 0.12 | 85.85–86.33 |
| *Prolemur simus* | Homozygote | Dichromat | L | 3 | 85.71 ± 0.02 | 85.67–85.75 |
| *Propithecus diadema* | Homozygote | Dichromat | L | 2 | 86.09 ± 0.06 | 86.05–86.13 |
| | Homozygote | Dichromat | M | 1 | 86.75 | N/A |
| | Heterozygote | Trichromat | L | 3 | 86.12 ± 0.14 | 86.02–86.28 |
| | | | M | | 86.68 ± 0.21 | 86.53–86.92 |
| *Propithecus edwardsi* | Homozygote | Dichromat | L | 7 | 85.94 ± 0.15 | 85.73–86.52 |
| | Homozygote[a] | Dichromat | L | 12 | 86.04 ± 0.11 | 85.78–86.27 |
| | Homozygote | Dichromat | M | 1 | 86.51 ± 0.03 | 86.48–86.53 |
| | Heterozygote | Trichromat | L | 4 | 85.96 ± 0.11 | 85.90–86.32 |
| | | | M | | 86.56 ± 0.12 | 86.45–86.90 |
| | Heterozygote[a] | Trichromat | L | 1 | 86.20 ± 0.08 | 86.12–86.27 |
| | | | M | | 86.82 ± 0.05 | 86.78–86.87 |
| *Propithecus verreauxi* | Homozygote | Dichromat | M | 8 | 86.48 ± 0.09 | 86.28–86.65 |
| *Varecia variegata* | Homozygote | Dichromat | L | 4 | 85.83 ± 0.12 | 85.67–86.07 |
| | Homozygote | Dichromat | M | 4 | 86.30 ± 0.06 | 86.20–86.40 |
| | Heterozygote | Trichromat | L | 5 | 85.80 ± 0.12 | 85.45–85.95 |
| | | | M | | 86.40 ± 0.12 | 86.13–86.60 |

Variance and range values include replicates

[a] Denotes samples derived from fecal DNA

likely to have multiple melting domains (Wittwer et al. 2003; personal observations), and allow for rapid thermal cycling (Wittwer et al. 2003). Qiagen recommends 70-350-bp amplicons, and we obtained differentiation with our target amplicon lengths of 166 bp (exon 3) and 240 bp (exon 5). Notably, however, SNVs have been successfully genotyped with amplicons up to 544-bp long (Wittwer et al. 2003).

2. Before implementing HRMA, sequence a subset of samples to characterize variation in the population, and to identify how melting temperatures correspond with genotypes. Opsin loci sometimes include multiple variable sites (e.g., Hiwatashi et al. 2010), which could complicate melting curves if linkage disequilibrium is incomplete or if variable sites represent point mutations. The free online program uMELT can be used to predict melting curve profiles based on a given sequence (Dwight et al. 2011), and thus to test whether genotypes will differ sufficiently without wasting reagents and templates.
3. Include positive controls and report reference melting temperatures for each genotype as these can vary slightly across labs and platforms (i.e., absolute melting temperatures may not be directly comparable). Moreover, although the reference curves were consistent across DNA sources (blood vs. feces), a test using whole genome amplifications (WGA) generated curves that were shifted slightly compared to genomic DNA from the same sample. Although melting curve patterns of WGAs were consistent with those generated using genomic DNA, peak melting temperatures differed, such that melting temperatures for WGA samples were generally higher compared to genomic DNA (note—all values in Table 2 are for genomic DNA). For example, mean melting temperature for the *E. rubriventer* L opsin is 86.37 ± 0.19 ($n = 7$; range 86.12–86.60) using WGAs compared to 85.56 ± 0.14 ($n = 8$; range 85.35–85.83) using genomic DNA from blood samples. As previous studies have found WGA products to result in higher rates of HRMA genotype misclassification compared to genomic DNA (Cho et al. 2008), projects using WGA products will likely require additional validation steps.

Because HRMA is an immediate post-PCR process utilizing real-time instrumentation, it removes the need for several downstream procedures, such as gel electrophoresis, PCR purification, and Sanger sequencing. Accordingly, not only is genotyping via HRMA rapid, it is also cost-effective. Although PCR cost per sample is slightly more expensive using HRMA than traditional PCR (e.g., Qiagen Type-it HRM kit results in an increase of ~$0.15/PCR

reaction compared to Qiagen HotStarTaq Master Mix), post-PCR processes can lead to additional costs ranging from hundreds to thousands of US dollars depending on the scale of the study (e.g., sequencing costs for 100 individuals at \$5/read is ~\$1000).

The utility of HRMA extends beyond studies of lemur color vision. The method could be useful for identifying color vision genotypes in polymorphic platyrrhines, and may also allow rapid and inexpensive screening for rare color vision variants in catarrhine populations using gene copy-specific primers (Vossen et al. 2009).

Finally, applications of this method may extend to other SNV genotyping studies in primates, such as identifying variation at loci associated with pathogen resistance [e.g., *FY/DARC* (Tung et al. 2009)], or screening for variation in dietary proteins [e.g., *APOE* (McIntosh et al. 2012)] and taste receptors [e.g., *TAS2R38* (Wooding et al. 2006)]. HRMA has also been successfully used for species identification (Ramón-Laca et al. 2014) and microsatellite analysis (Thomsen et al. 2012) in other taxa. Thus, the approach we describe here has the potential for broad application in genetic studies of primate populations.

**Acknowledgments** We thank Shoji Kawamura, Amanda Melin, and Michael James Montague for helpful comments and suggestions, and we thank Gary Aronsen for logistical support in the Yale Molecular Anthropology Lab. Funding was provided by the National Science Foundation (FSML 1227143), the UK Natural Environment Research Council, Yale University, and the George Washington University. All applicable international, national, and institutional guidelines for the care and use of animals were followed. The authors declare that they have no conflict of interest.

## References

Bowmaker JK, Dartnall HJA, Mollon JD (1980) Micro-spectrophotometric demonstration of 4 classes of photoreceptor in an Old World primate, *Macaca fascicularis*. J Physiol Lond 298:131–143

Bunce JA, Isbell LA, Neitz M, Bonci D, Surridge AK, Jacobs GH, Smith DG (2011) Characterization of opsin gene alleles affecting color vision in a wild population of titi monkeys (*Callicebus brunneus*). Am J Primatol 73:189–196

Cho MH, Ciulla D, Klanderman BJ, Raby BA, Silverman EK (2008) High resolution melting curve analysis of genomic and whole genome amplified DNA. Clin Chem 54:2055–2058

Dacey DM (2000) Parallel pathways for spectral coding in primate retina. Annu Rev Neurosci 23:743–775

Doktycz MJ (2002) Nucleic acids: thermal stability and denaturation. Wiley, Chichester. http://www.els.net. doi:10.1038/npg.els.0003123

Dulai KS, von Dornum M, Mollon JD, Hunt DM (1999) The evolution of trichromatic color vision by opsin gene duplication in New World and Old World primates. Genome Res 9:629–638

Dwight Z, Palais R, Wittwer CT (2011) uMELT: prediction of high-resolution melting curves and dynamic melting profiles of PCR products in a rich web application. Bioinformatics 27:1019–1020

Fedigan L, Melin AD, Addicott J, Kawamura S (2014) The heterozygote superiority hypothesis for polymorphic color vision is not supported by long-term fitness data from wild Neotropical monkeys. PLoS One 9:e84872

Hiramatsu C, Tsutsui T, Matsumoto Y, Aureli F, Fedigan LM, Kawamura S (2005) Color vision polymorphism in wild capuchins (*Cebus capucinus*) and spider monkeys (*Ateles geoffroyi*) in Costa Rica. Am J Primatol 67:447–461

Hiramatsu C, Melin AD, Aureli F, Schaffner CM, Vorobyev M, Matsumoto Y, Kawamura S (2008) Importance of achromatic contrast in short-range fruit foraging in primates. PLoS One 3:e3356

Hiwatashi T, Okabe Y, Tsutsui T, Hiramatsu C, Melin AD, Oota H, Schaffner CM, Aureli F, Fedigan LM, Innan H, Kawamura S (2010) An explicit signature of balancing selection for color vision variation in New World monkeys. Mol Biol Evol 27:453–464

Jacobs GH (1984) Within species variations in visual capacity among squirrel monkeys (*Saimiri sciureus*) color vision. Vision Res 24:1267–1277

Jacobs GH (1993) The distribution and nature of color vision among the mammals. Biol Rev Camb Philos 68:413–471

Jacobs GH (1995) Variations in primate color vision: mechanisms and utility. Evol Anthropol 3:196–205

Jacobs GH (1998) A perspective on color vision in platyrrhine monkeys. Vis Res 38:3307–3313

Jacobs RL, Bradley BJ (2016) Considering the influence of nonadaptive evolution on primate color vision. PLoS One 11:e0149664. doi:10.1371/journal.pone.0149664

Jacobs GH, Deegan JF (2003) Photopigment polymorphism in prosimians and the origins of primate trichromacy. In: Mollon JD, Pokorny J, Knoblauch K (eds) Normal and defective colour vision. Oxford University Press, Oxford, pp 14–20

Leonhardt SD, Tung J, Camden JB, Leal M, Drea CM (2009) Seeing red: behavioral evidence of trichromatic color vision in strepsirrhine primates. Behav Ecol 20:1–12

Liew M, Pryor R, Palais R, Meadows C, Erali M, Lyon E, Wittwer C (2004) Genotyping of single-nucleotide polymorphisms by high-resolution melting of small amplicons. Clin Chem 50:1156–1164

McIntosh A, Bennett C, Dickson D, Anestis SF, Watts DP, Webster TH, Fontenot MB, Bradley BJ (2012) The apolipoprotein E (*APOE*) gene appears functionally monomorphic in chimpanzees (*Pan troglodytes*). PLoS One 7:e47760

Melin AD, Fedigan LM, Hiramatsu C, Sendall CL, Kawamura S (2007) Effects of colour vision phenotype on insect capture by a free-ranging population of white-faced capuchins, *Cebus capucinus*. Anim Behav 73:205–214

Melin AD, Fedigan LM, Hiramatsu C, Kawamura S (2008) Polymorphic color vision in white-faced capuchins (*Cebus capucinus*): is there foraging niche divergence among phenotypes? Behav Ecol Sociobiol 62:659–670

Mundy NI, Morningstar NC, Baden AL, Fernandez-Duque E, Bradley BJ (2016) Can colour vision re-evolve? Variation in the X-linked opsin locus of cathemeral Azara's owl monkeys (*Aotus a. azarae*). Front Zool 13:9. doi:10.1186/s12983-016-0139-z

Nathans J (1999) The evolution and physiology of human color vision: insights from molecular genetic studies of visual pigments. Neuron 24:299–312

Nathans J, Thomas D, Hogness DS (1986) Molecular genetics of human color vision: the genes encoding blue, green, and red pigments. Science 232:193–202

Neitz M, Neitz J, Jacobs GH (1991) Spectral tuning of pigments underlying red-green color vision. Science 252:971–974

Parant JM, George SA, Pryor R, Wittwer CT, Yost HJ (2009) A rapid and efficient method of genotyping zebrafish mutants. Dev Dyn 238:3168–3174

Payne MS, Tabone T, Kemp MW, Keelan JA, Spiller OB, Newnham JP (2014) High-resolution melt PCR analysis for genotyping of

*Ureaplasma parvum* isolates directly from clinical samples. J Clin Microbiol 52:599–606

Ramón-Laca A, Gleeson D, Yockney I, Perry M, Nugent G, Forsyth DM (2014) Reliable discrimination of 10 ungulate species using high resolution melting analysis of faecal DNA. PLoS One 9:e92043

Shyue SK, Boissinot S, Schneider H, Sampaio I, Schneider MP, Abee CR, Williams L, Hewett-Emmett D, Sperling HG, Cowing JA, Dulai KS, Hunt DM, Li W-H (1998) Molecular genetics of spectral tuning in New World monkey color vision. J Mol Evol 46:697–702

Smith BL, Lu CP, Bremer JRA (2010) High-resolution melting analysis (HRMA): a highly sensitive inexpensive genotyping alternative for population studies. Mol Ecol Resour 10:193–196

Smith AC, Surridge AK, Prescott MJ, Osorio D, Mundy NI, Buchanan-Smith HM (2012) The effect of colour vision status on insect prey capture efficiency by captive and wild tamarins (*Saguinus* spp.). Anim Behav 83:479–486

Surridge AK, Osorio D, Mundy NI (2003) Evolution and selection of trichromatic vision in primates. Trends Ecol Evol 18:198–205

Surridge AK, Suárez SS, Buchanan-Smith HM, Mundy NI (2005) Non-random association of opsin alleles in wild groups of red-bellied tamarins (*Saguinus labiatus*) and maintenance of the colour vision polymorphism. Biol Lett 1:465–468

Tan Y, Li WH (1999) Vision—trichromatic vision in prosimians. Nature 402:36

Thomsen N, Ali RG, Ahmed JN, Arkell RM (2012) High-resolution melt analysis (HRMA); a viable alternative to agarose gel electrophoresis for mouse genotyping. PLoS One 7:e45252

Tovee MJ (1994) The molecular genetics and evolution of primate color vision. Trends Neurosci 17:30–37

Tung J, Primus A, Bouley AJ, Severson TF, Alberts SC, Wray GA (2009) Evolution of a malaria resistance gene in wild primates. Nature 460:388–391

Valenta K, Edwards M, Rafaliarison RR, Johnson SE, Holmes SM, Brown KA, Dominy NJ, Lehman SM, Parra EJ, Melin AD (2015) Visual ecology of true lemurs suggests a cathemeral origin for the primate cone opsin polymorphism. Funct Ecol. doi:10.1111/1365-2435.12575

Veilleux CC, Bolnick DA (2009) Opsin gene polymorphism predicts trichromacy in a cathemeral lemur. Am J Primatol 71:86–90

Veilleux CC, Jacobs RL, Cummings ME, Louis EE, Bolnick DA (2014) Opsin genes and visual ecology in a nocturnal folivorous lemur. Int J Primatol 35:88–107

Vogel ER, Neitz M, Dominy NJ (2007) Effect of color vision phenotype on the foraging of wild white-faced capuchins, *Cebus capucinus*. Behav Ecol 18:292–297

Vossen RHAM, Aten E, Roos A, den Dunnen JT (2009) High-resolution melting analysis (HRMA): more than just sequence variant screening. Hum Mutat 30:860–2866

Wittwer CT, Reed GH, Gundry CN, Vandersteen JG, Pryor RJ (2003) High-resolution genotyping by amplicon melting analysis using LCGreen. Clin Chem 49:853–860

Wooding S, Bufe B, Grassi C, Howard MT, Stone AC, Vazquez M, Dunn DM, Meyerhof W, Weiss RB, Bamshad MJ (2006) Independent evolution of bitter-taste sensitivity in humans and chimpanzees. Nature 440:930–934

Yokoyama S, Radlwimmer FB (1998) The "five-sites" rule and the evolution of red and green color vision in mammals. Mol Biol Evol 15:560–567